Electrons and cavitation in liquid helium

J. Classen,* C.-K. Su, M. Mohazzab,† and H. J. Maris
Department of Physics, Brown University, Providence, Rhode Island 02912
(Received 17 April 1997)

We describe a number of experiments in which the effect of electrons on cavitation is studied. Electrons in liquid helium become trapped in a bubble from which the liquid is almost completely excluded. By applying a negative pressure to the helium, we are able to make these bubbles explode. We have measured the variation of this pressure with temperature and the results are in very good agreement with theoretical expectations. At low temperatures the electron bubbles become attached to vortices. The circulation of the liquid around the electron bubble leads to a reduction in the magnitude of the negative pressure required to explode the bubble, and we have been able to measure this reduction. [S0163-1829(98)05806-8]

I. INTRODUCTION

A number of recent experiments have studied the nucleation of bubbles in liquid helium, both in the normal and the superfluid phases.[1–3] Liquid helium is an attractive material in which to perform nucleation studies. The liquid can be prepared in a state of unusually high purity. Because helium does not freeze even at absolute zero, quantum nucleation processes can also be investigated.[4–6] Most of the experiments that have been performed use a focused sound wave to produce an oscillating pressure within a small volume of liquid. Light-scattering techniques are then used to detect the nucleation of bubbles in the vicinity of the acoustic focus.

It is believed that in these experiments one is studying homogeneous nucleation, i.e., nucleation unaffected by the influence of any impurities in the liquid. However, one can also consider the introduction into the liquid of various impurities which might affect the nucleation process. The list of impurities includes electrons, positive helium ions, helium molecules in an excited state, and ions and neutral atoms of other elements. In addition, in the superfluid state it is possible that the nucleation is influenced by the presence of quantized vortices.[7]

In this paper we report on a series of experiments we have performed to study the effect of electrons on cavitation in liquid helium. It is well known that when an electron enters liquid helium it forms a spherical cavity in the liquid from which the helium atoms are almost completely excluded. The size of this cavity is determined by a balance between the quantum-mechanical zero-point energy of the electron, the surface energy of the cavity wall, and the effects of the applied pressure. When a negative pressure is applied to the liquid the existence of these ''electron bubbles'' can greatly increase the probability that cavitation will occur. Preliminary reports of measurements of electron-induced cavitation have been made in Refs. 8 and 9. In Sec. II we work out the theory of this process, and the experiments and results are described in Secs. III and IV.

II. THEORY

A. Simple theory of the barrier

An electron entering helium experiences a repulsive potential V_0. Experiments indicate that this potential is approximately 1.0 eV.[10] Once the electron is inside the liquid it is energetically favorable for it to become localized within a spherical volume from which the helium is almost completely excluded. As a first approximation one can consider that the energy E of the electron bubble is the sum of the zero-point energy of the electron, the surface energy of the bubble, and a volume energy proportional to the applied pressure P, i.e.,

$$E=\frac{h^2}{8mR^2}+4\pi R^2\alpha+\frac{4}{3}\pi R^3P, \tag{1}$$

where R is the bubble radius, m is the electron mass, and α is the surface energy per unit area.[11] At zero pressure the radius at which the energy is a minimum is

$$R_{\min}=\left(\frac{h^2}{32\pi m\alpha}\right)^{1/4}. \tag{2}$$

This radius is 19 Å at $T=0$ and increases slightly as the temperature goes up because of the decrease in the surface tension. In writing down Eq. (1) it is assumed that the energy of the electron is much less than the barrier height V_0, so that the penetration of the electron into the bubble wall is unimportant. In a more sophisticated theory several other effects can be included. The influence of these is discussed below.

The application of a positive pressure makes the equilibrium size of the bubble decrease. When the pressure is negative the radius $R_{\min}$ at which the minimum energy occurs becomes larger. This bubble size no longer corresponds to a global minimum of the energy. For R greater than $R_{\min}$ the energy passes through a maximum at $R_{\max}$ and then decreases monotonically, eventually becoming negative. If the magnitude of the negative pressure is increased, $R_{\min}$ and $R_{\max}$ approach each other. Finally, for pressures more negative than a critical value P_c there is no longer an energy minimum and the bubble becomes unstable. This pressure is given by

$$P_c=-\frac{16}{5}\left(\frac{2\pi m}{5h^2}\right)^{1/4}\alpha^{5/4}. \tag{3}$$

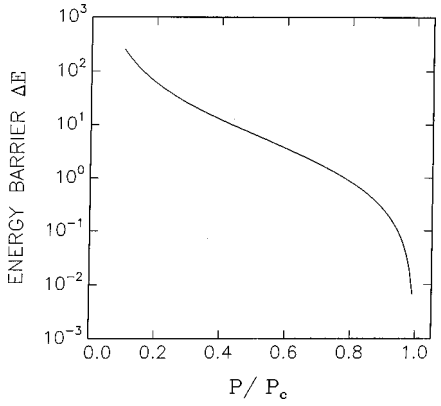

FIG. 1. Plot of the energy barrier ΔE as a function of the pressure divided by the pressure P_c at which the electron bubble explodes. The barrier is plotted in units of $(h^2\alpha/m)^{1/2}$ where α is the surface tension of the liquid and m is the mass of an electron.

At zero temperature and using the value 0.3544 erg cm^{-2} for α (Ref. 12) this gives an instability pressure of -1.98 bars. In the range of pressures before P_c is reached an energy barrier must be overcome before nucleation can occur. The height of this energy barrier is

$$\Delta E = E(R_{\max}) - E(R_{\min}). \tag{4}$$

One cannot calculate this barrier in closed form for an arbitrary pressure. However, one can express the barrier in the form

$$\Delta E = \left(\frac{h^2\alpha}{m}\right)^{1/2} g(P/P_c), \tag{5}$$

where g is a function that can be determined numerically. The calculated barrier as a function of P/P_c is shown in Fig. 1.

For P close to P_c it is straightforward to show that

$$R_{\min} = R_c\left[1 - \left(\frac{2(P-P_c)}{5|P_c|}\right)^{1/2} + \cdots\right], \tag{6}$$

$$R_{\max} = R_c\left[1 + \left(\frac{2(P-P_c)}{5|P_c|}\right)^{1/2} + \cdots\right]. \tag{7}$$

In this range of pressures the energy barrier is

$$\Delta E = \frac{32}{15}\left(\frac{\pi h^2\alpha}{m}\right)^{1/2}\left(\frac{P-P_c}{|P_c|}\right)^{3/2}. \tag{8}$$

The probability Γ per unit time that as a result of thermal fluctuations an electron bubble will overcome the energy barrier and a macroscopic bubble will nucleate is

$$\Gamma = \Gamma_0 \exp(-\Delta E/k_B T), \tag{9}$$

where Γ_0 is the attempt frequency and T is the temperature. If the liquid contains n electrons per unit volume, and a negative pressure P is applied to a volume $V_{\exp}$ for a time $\tau_{\exp}$, the probability that at least one bubble will nucleate is then

$$S = 1 - \exp[-nV_{\exp}\tau_{\exp}\Gamma_0 \exp(-\Delta E/k_B T)]. \tag{10}$$

We can expect that the attempt frequency will be of the order of $k_B T/h$, i.e., of the order of magnitude of 10^{11} s^{-1}. In the experiments that we have performed the number density of the electrons is usually less than 10^6 cm^{-3}. If we take the experimental volume to be $(\lambda/2)^3$ which is $\sim 10^{-5}$ cm^3 for a frequency of 560 kHz and the experimental time to be $\sim 10^{-5}$ s, then $nV_{\exp}\tau_{\exp}\Gamma_0$ is of the order of 10^7. It follows that there is an appreciable probability (e.g., $S \sim 0.5$) of nucleation only if the energy barrier is sufficiently small that $\exp(-\Delta E/k_B T) > 10^{-7}$, i.e., if $\Delta E \leqslant 16 k_B T$. This, in turn means that for nucleation to occur the ratio of the pressure P to the critical pressure P_c must be such that the function g has a value less than

$$g_c \sim \frac{16 k_B T}{h}\left(\frac{m}{\alpha}\right)^{1/2}. \tag{11}$$

Using the known temperature dependence of the surface energy, one obtains values of g_c of 0.02, 0.04, and 0.12 at temperatures of 1, 2, and 4 K, respectively. From the calculated function $g(P/P_c)$ one can find that nucleation only occurs within 2, 3, and 7% of P_c at these three temperatures. As a consequence, it is not always necessary to consider the value of the nucleation barrier as a function of pressure, and the quantity of primary interest is simply the value of the critical pressure.

B. Effect of barrier penetration and polarizability

The simple theory can be corrected to allow for the finite height of the potential barrier that confines the electron within the bubble. Penetration of the electron wave function into the liquid helium lowers the zero-point energy of the electron. Consequently, the equilibrium size of the electron bubble for a given negative pressure will be decreased and the nucleation barrier will increase. To make a rough estimate of the magnitude of this effect we need a value for the potential energy of interaction between an electron and liquid helium. There are a number of experimental and theoretical investigations of this quantity.[11] For simplicity, we have assumed that for helium with a density that corresponds to zero temperature and zero pressure ($\rho = 0.14513$ g cm^{-3}) the potential is 1 eV, and that the potential is proportional to the liquid density. The calculation of the energy barrier for nucleation is straightforward, and the results for zero temperature are shown in Fig. 2. Included in this figure are the results from the simple theory with an impenetrable barrier. It can be seen that the effect of the penetration of the wave function into the helium gives only a very small correction to the nucleation barrier. The instability pressure is increased from -1.98 to -2.08 bars.

A second correction arises from the polarizability of the liquid. This gives a contribution to the energy which is[11]

$$E_{\text{pol}} = -\frac{(\epsilon - 1)e^2}{2\epsilon R}, \tag{12}$$

where ϵ is the dielectric constant of helium. For liquid at zero pressure and zero temperature $\epsilon = 1.0573$. Inclusion of the polarization contribution to the energy gives the results shown in Fig. 2. The instability pressure is increased to -2.19 bars.

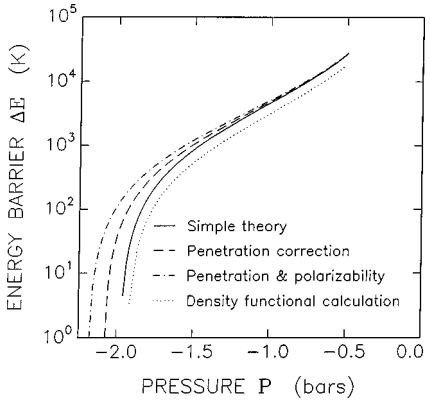

FIG. 2. The nucleation barrier as a function of pressure at zero temperature. The solid line is the result of the simple theory [Eq. (1)]. The dashed curve shows the effect of the penetration of the electron wave function into the liquid. The dashed-dotted line indicates the effect of inclusion of the polarizability of the helium and the penetration of the wave function into the liquid. The dotted line is the result obtained when a density-functional theory is used to describe the liquid. The density-functional theory does not include the effects of the polarizability of the liquid.

C. Effect of finite wall thickness

The radius of the bubble at the instability pressure is approximately 29 Å at $T=0$ K. This compares with the width of the liquid-gas interface which has been measured to be 9 Å.[13] To allow for the finite width of the helium wall we use a density-functional scheme to describe the helium.[7] The free energy of nonuniform helium is taken to be

$$\int [f(\rho)+\lambda|\nabla\rho|^2]dV, \tag{13}$$

where $f(\rho)$ is the energy per unit volume of uniform liquid when the density is ρ, and the second term is the extra energy associated with density gradients. In this scheme f is determined by extrapolation of the measured properties of the liquid at positive pressures, and the value of the parameter λ is fixed by the requirement that the model gives the correct value for the surface energy. Note that the pressure of the liquid is related to the density by

$$P=-f+\rho\frac{\partial f}{\partial\rho}. \tag{14}$$

When Eq. (13) is used for the calculation of the energy required to form a bubble it is necessary to perform the integral over the entire volume of the liquid, not just the region containing the bubble. This is because the helium that is removed from the bubble region has to be redistributed over the volume of the remaining liquid. The increase in the energy of helium relative to the energy of the same mass of helium but with uniform density ρ_1 is

$$E_{\rm hel}=\int [\phi(\rho,\rho_1)+\lambda|\nabla\rho|^2]dV, \tag{15}$$

where $\phi(\rho,\rho_1)\equiv f(\rho)-f(\rho_1)-(\rho-\rho_1)f'(\rho_1)$. This form has the advantage that the energy of the bubble can be calculated by an integral extending only over the bubble region.

For the interaction energy between the electron and the liquid helium we use the local interaction

$$E_{\rm int}=U_0\int|\psi|^2\rho dV. \tag{16}$$

The coefficient U_0 is chosen so that the energy barrier encountered by an electron entering helium has the correct value. This gives $U_0=1.1\times10^{-11}$ erg g^{-1} cm^3.

We are interested in finding the lowest energy state of the electron bubble and also the wave function and density distribution that corresponds to the critical nucleus. For both the lowest energy and the nucleation state, the total energy must be stationary with respect to any variation in the electron wave function and the helium density. It follows that $\psi(r)$ and $\rho(r)$ must satisfy the coupled equations (but see comment below)

$$U_0|\psi|^2+f'(\rho)-f'(\rho_1)-2\lambda\nabla^2\rho=0, \tag{17}$$

$$-\frac{\hbar^2}{2m}\nabla^2\psi+U_0\rho\psi=E_{\rm el}\psi. \tag{18}$$

$E_{\rm el}$ is the energy eigenvalue for the electron. The boundary conditions on the electron wave function are $\psi'=0$ at the center of the bubble ($r=0$) and $\psi=0$ as $r\to\infty$. The gradient of the density must vanish at $r=0$, and the density must tend to the bulk value ρ_1 as $r\to\infty$. In addition, the solution for ψ must be such that the wave function is normalized. Because the density $\rho(r)$ can never be negative it follows that Eq. (17) is to be applied only when $\rho(r)$ is nonzero. One can see this in a formal way by writing $\rho(r)=A(r)^2$ with $A(r)$ real so as to force ρ to be non-negative. A variation of the total energy with respect to the field $A(r)$ then gives the same result as in Eq. (17) but multiplied by an extra factor of $A(r)\equiv\rho(r)^{1/2}$. Hence, to have a stationary energy one requires *either* that Eq. (17) hold *or* that $\rho(r)=0$.

At first sight it would appear that these equations could be solved by choosing trial values of ψ and ρ at $r=0$, together with the electron energy $E_{\rm el}$, and then adjusting these choices so that when ψ and ρ are integrated out to large r the correct limiting values are obtained. One finds, however, that this procedure does not work because with the form of density functional that we are using the value of ρ at the origin is exactly zero. The density is zero out to some finite radius $r_{\rm start}$, and then varies quadratically with distance for r slightly greater than this value. The procedure to find the solution is then as follows. As a first step a guess is made for the parameters $\psi(r=0)$, $r_{\rm start}$, and $E_{\rm el}$. Then the Schrödinger equation (18) can be solved analytically in the range from $r=0$ to $r=r_{\rm start}$. This gives values of $\psi(r_{\rm start})$ and $(\partial\psi/\partial r)_{r=r_{\rm start}}$. We then numerically integrate Eqs. (17) and (18) starting at $r=r_{\rm start}$ and going to larger values of r. The values of $\psi(r=0)$, $r_{\rm start}$, and $E_{\rm el}$ are then adjusted so that at a large distance ψ goes to zero, ρ tends to ρ_1, and the integral of $|\psi|^2$ is unity. Typically we have performed the numerical integration with a step size of 0.5 Å and have continued the integration out to a distance r about twice the radius of the bubble. Thus, an appropriate choice of parameters is $\psi(r=0)$, $r_{\rm start}$, and $E_{\rm el}$.

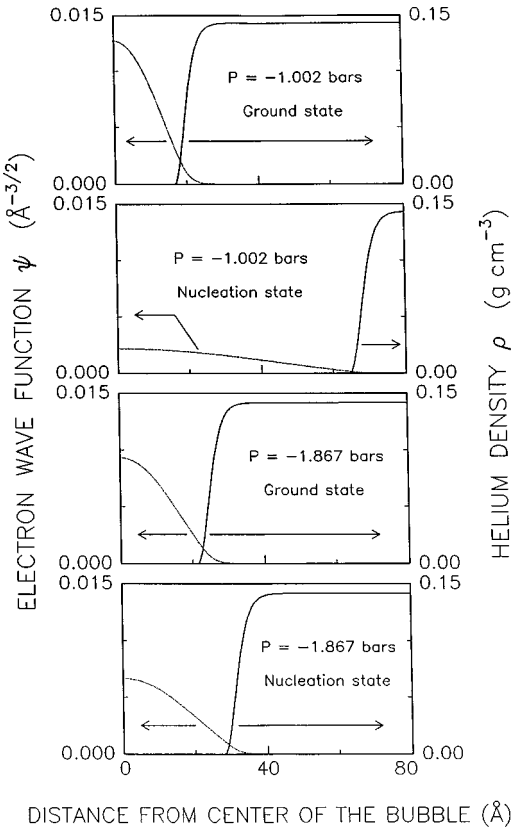

FIG. 3. The electron wave function ψ and the helium density ρ as a function of the distance from the center of the bubble for the ground and nucleation states at $P=-1.002$ and $P=-1.867$ bars. The temperature is zero.

When this procedure is carried out, one finds a number of different types of solutions. One family of solutions corresponds physically to the electron being in one of the sequence of states with different radial quantum numbers n and S symmetry, with the size of the bubble and the profile of the helium density in the wall arranged to minimize the energy. A second family are ''nucleation solutions'' and correspond to the configuration of the electron and the liquid at the highest point on the energy barrier. These nucleation solutions also have S symmetry. Let us denote the energies of the lowest energy $(n=1)$ solutions of these two types by E_g and E_n, respectively. Then the energy barrier is

$$\Delta E = E_g - E_n . \tag{19}$$

The results of a calculation of the energy barrier at zero temperature made by this method are shown in Fig. 2. This calculation ignores the contribution to the energy arising from the polarizability of the helium. It can be seen that the effect of the finite wall thickness is to lower the energy barrier. The pressure at which the bubble becomes unstable is reduced from -2.08 bars, the result for a sharp liquid interface and allowing for electron penetration, to -1.92 bars. The form of the electron wave function and the helium wall profile are shown in Fig. 3 for $P=-1.002$ bars and for $P=-1.867$ bars.

D. Effect of finite temperature

For finite temperatures a number of new physical effects enter. These include the temperature dependence of the surface energy and of the density of the liquid, and the possible presence of some helium vapor inside the bubble. In principle, the influence of these effects on the energy barrier can be calculated through the use of Eqs. (17) and (18). An estimate of the free energy, the density-functional parameter λ, and other thermodynamic properties of liquid helium at negative pressures has recently been made.[14] The estimates were made for a series of temperatures in the range 2.41–4.21 K. We have attempted to use these estimates in Eqs. (17) and (18) to obtain the energy barrier. However, we had great difficulty in obtaining satisfactory solutions of the coupled differential equations, as a result of the number of numerical instabilities that occur.

As a consequence, we have looked for a simpler method. We first note that the results of the zero-temperature density-functional calculation do not differ greatly from a simpler theory in which the liquid is taken to have an abrupt interface. In addition, the effect of the penetration of the electron wave function into the liquid is small. Accordingly, we have calculated the barrier in terms of a simplified model in which it is assumed that outside a radius r_1 the density of the helium equals the density of bulk liquid. The region inside the radius r_1 contains the electron and helium gas. The total energy is taken to be

$$E = -\int_0^{r_1} \frac{\hbar^2}{2m}\,\psi\nabla^2\psi 4\pi r^2 dr + \int_0^{r_1} \phi_g(r) 4\pi r^2 dr + \int_0^{r_1} U_0|\psi|^2 \rho_g(r)\pi r^2 dr + 4\pi r_1^2 \alpha, \tag{20}$$

where $\rho_g(r)$ is the density of gas at distance r from the center, and $\phi_g(r)$ is the corresponding value of ϕ. The wave function of the electron is required to go to zero at $r=r_1$, and the surface energy of the liquid per unit area is assumed to be α, regardless of the value of the gas density at $r=r_1$. Let us suppose that a value for r_1 has been chosen. Minimization of E with respect to variation of $\psi(r)$ then yields the Schrödinger equation Eq. (18). Minimization with respect to variations in the density of the gas gives the condition

$$U_0\psi^2 + f'(\rho_g) - f'(\rho_1) = 0. \tag{21}$$

This is identical to Eq. (17) except for the absence of the term in $\nabla^2\rho$. We come back to this point briefly below.

To minimize the energy we proceed as follows. We first calculate the electron wave function with the gas density set equal to zero. Using the calculated ψ we then find the gas density from Eq. (21). To do this we treat the gas as ideal which enables us to write[14]

$$f_g = \frac{\rho_g k_B T}{M}\,[\ln(\rho_g/\rho_Q) - 1]. \tag{22}$$

In this result $\rho_Q = M(Mk_BT/2\pi\hbar^2)^{3/2}$ and M is the mass of a helium atom. Combining Eqs. (21) and (22) gives the gas density in the closed form

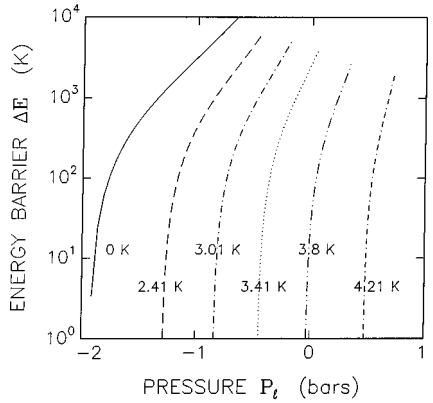

FIG. 4. The nucleation barrier as a function of pressure and temperature. The results for $T=0$ are calculated using the density-functional scheme. The results for finite T are based on the simplified model in which the penetration of the electron wave function into the liquid helium is ignored, and the energy of the bubble is as given by Eq. (20).

$$\rho_g(r)=\rho_Q \exp\left\{\frac{M}{k_B T}[f'(\rho_1)-U_0|\psi(r)|^2]\right\}. \qquad (23)$$

The wave function is then recalculated from Eq. (18) using the gas density just determined and the procedure repeated until convergence is achieved. The calculation is repeated for a range of values of r_1, and the energies of the ground and the nucleation states are determined.

The results for the energy barrier as a function of temperature and pressure are included in Fig. 4. As examples, the wave function and density profile calculated for two pressures at 4.21 K are shown in Fig. 5. An interesting feature of the results is that in the higher part of the temperature range nucleation occurs at a pressure which is *positive*. At these temperatures the critical nucleus has the electron confined in a central core and surrounded by a gas layer.

As already mentioned, in the calculation just performed there is no term in the equation for the gas density that involves $\nabla^2\rho_g$. If such a term were included it might still be possible to solve the coupled equations for ψ and ρ by means of an iteration method similar to the one just described. We have not attempted this. In fact, it is not clear to us that the density-functional scheme we are using is appropriate for this application. The parameter λ is fixed by requiring that the density functional give the correct value for the energy of the liquid-gas interface. This means that λ is chosen such that

$$\alpha(T)=2\int_{\rho_{gSVP}}^{\rho_{lSVP}}[\lambda(T)\phi(\rho,\rho_{lSVP})]^{1/2}d\rho, \qquad (24)$$

where ρ_{gSVP} and ρ_{lSVP} are the densities of gas and liquid at the liquid-gas coexistence pressure for temperature T. If one examines the integrand one finds that the main contribution to the integral comes from the density range from ~ 0.2 to ~ 0.8 of the full liquid density. Consequently, we have no reason to believe that the energetics of an inhomogeneous *low-density* gas are well described by the form of the density functional that we have used. It might, in fact, be more appropriate to use an approach in which the quantum states of helium atoms moving in the potential energy resulting from

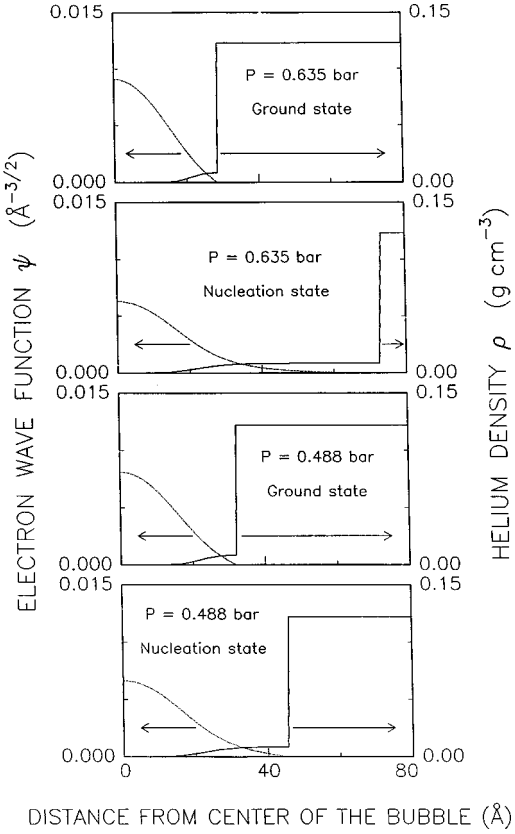

FIG. 5. The electron wave function ψ and the helium density ρ as a function of the distance from the center of the bubble for the ground and nucleation states at $P=0.635$ and $P=0.488$ bars. The temperature is 4.21 K.

the interaction with the electron are evaluated, and then helium atoms are placed in these states according to a Bose-Einstein distribution. The effective potential for a gas atom moving inside the bubble is $U_0\psi^2 M$.

Neglect of the term in $\nabla^2\rho_g$ is equivalent to the assumption that the density distribution in the gas is well approximated by classical statistical mechanics. This appears to be a reasonable approximation in the present context since the effects of the gas are only important in the higher part of the temperature range. At 4.21 K, for example, the momentum of a helium atom of average thermal energy $3k_BT/2$ is 1.1×10^{-19} g cm s^{-1}. On the other hand, one can see from Fig. 5 that the characteristic distance ζ over which the density of the gas changes is larger for the nucleation state than for the ground state, but is typically in the range 5–20 Å. By the uncertainty principle this density variation forces atoms in the gas to have momenta $\hbar/\zeta$ of the order of 10^{-20} g cm s^{-1}. Hence it is significantly less than the momentum of the average thermal energy. Thus quantum effects do not appear to be large.

E. Effect of quantized vortices

At sufficiently low temperatures electron bubbles attach themselves to quantized vortices. Because of the liquid circulation around the vortex one expects that the energy barrier for nucleation will be reduced relative to the barrier for an electron bubble in bulk liquid at the same pressure. Quantized vortices exist only in the superfluid phase, and in this

temperature range the effect of gas on the nucleation process is very small. Hence, we take the energy of the electron bubble to be given by

$$E = E_{\rm el} + A\alpha + PV - \int \frac{1}{2}\rho_1 v^2 dV, \tag{25}$$

where $E_{\rm el}$ is the electron energy, A is the surface area of the bubble, V is its volume, and ρ_1 is the density of the liquid which is assumed to be a constant. The last term represents the decrease in the kinetic energy of the liquid which takes place when the axis of the bubble lies along the line of the vortex and the empty bubble displaces moving liquid. v is the circulation velocity which equals $\hbar/Mr$, with r the distance from the vortex. The vortex is assumed to be straight. It is necessary to modify the integrand of the kinetic energy integral in order to avoid a divergence at the vortex core. Donnelly and Roberts[15] have done this by modifying the liquid density according to the relation

$$\rho(r) = \rho_1 \frac{r^2}{r^2+\chi^2}, \tag{26}$$

where χ is 1.46 Å.

When the electron bubble is attached to a vortex, the bubble will no longer be spherical and the exact calculation of the energy barrier becomes very difficult. To obtain an approximate solution we have done the following. We neglect the penetration of the electron wave function into the helium. We then assume that the shape of the bubble can be taken to be a prolate spheroid with the semimajor axis a along the vortex and the semiminor axis b. The surface area is then

$$A = 2\pi\{b^2 + a^2 b \sin^{-1}[(a^2-b^2)^{1/2}/a]/(a^2-b^2)^{1/2}\}, \tag{27}$$

and the volume is $4\pi a b^2/3$. Evaluation of the term in Eq. (25) representing the kinetic energy of the displaced liquid gives the result

$$-\frac{\pi\rho_1\hbar^2 a}{M^2}\left[\zeta \ln\left(\frac{\zeta+1}{\zeta-1}\right) - 1\right], \tag{28}$$

where $\zeta = (1+\chi^2/b^2)^{1/2}$.

As a first approximation we consider a spherical bubble. The bubble becomes unstable at a pressure of -1.90 bars, compared to -1.98 bars without a vortex, a 4% decrease. In the second approximation we consider a prolate spheroid with $(1-b/a) \ll 1$. To first order in the parameter $(1-b/a)$ the energy of the electron is then

$$E_{\rm el} = \frac{h^2}{8ma^2}\left[1 + \frac{4}{3}\left(1 - \frac{b}{a}\right)\right]. \tag{29}$$

We then consider the stability of the bubble, allowing both a and b to vary. To within an accuracy of 0.01 bars we find that the instability occurs at the same pressure for a prolate spheroid as for a spherical bubble. We find that close to the instability pressure a is approximately 9% larger than b.

III. EXPERIMENT

The experimental setup was similar to that used in our earlier experiments.[8] An ultrasonic transducer was used to generate focused sound waves. If a bubble nucleated during the negative part of the pressure swing at the acoustic focus this could be detected by the light that was scattered from a laser beam focused onto the same spatial region.

The sample cell contained approximately 9 $\rm cm^3$ of liquid helium, and had two sapphire windows on opposite sides. The cell could be pressurized to at least 30 bars. Helium from a gas cylinder at room temperature was introduced into the low-temperature cylindrical experimental cell via a capillary. Measurements could be made over the temperature range from about 0.65 to 5 K.

Hemispherical piezoelectric transducers supplied by Channel Inc.[16] were used to generate sound. In most of the experiments the transducer was driven in the radial thickness mode of oscillation. In a first set of experiments a transducer (transducer A) of outer radius 1 cm and resonance frequency 560 kHz was used. Measurements were also made with a 0.95 cm radius transducer (transducer B) of frequency 1.4 MHz. This higher frequency transducer had the advantage that a smaller voltage was required in order to produce a given negative pressure swing at the focus. The transducer was mounted with its concave side facing down, and was supported by four short copper posts protruding from the inner wall of the cell and making contact with the lower edge of the transducer. The transducer was driven by rf pulses produced by feeding the output of a frequency synthesizer into a gated amplifier.

Electrons were introduced into the liquid by means of a 10 μCi ^{204}Tl β source. This source produces a continuous spectrum with a maximum electron energy of 764 keV. The electrons lose energy by excitation and ionization of the atomic electrons of helium while they travel at high velocity, and then form electron bubbles at the end of their range. The stopping range varies with energy and has a maximum value of 2.5 cm. The β source was located approximately 0.4 cm below the acoustic focus. The density distribution of the electrons in the cell could be modified by the application of a dc bias voltage $V_{\rm dc}$ to the inner concave surface of the transducer. The outer surface of the transducer, the β source and the cell wall were grounded.

A 10 mW He-Ne laser beam was passed through the acoustic focus and the light that was scattered was detected by means of a photomultiplier tube (PMT). The PMT was placed at an angle of around 10 mrad from the direction of the laser beam and had a time resolution of $\sim$100 ns.

IV. RESULTS AND DISCUSSION

A typical experiment consisted of the application of a series of rf pulses to the transducer and the determination of the number of times that a bubble was produced as indicated by scattered light reaching the photomultiplier. These results give the probability S of nucleation. Representative results for S as a function of the ac voltage $V_{\rm ac}$ applied to the transducer and the dc voltage $V_{\rm dc}$ are shown in Fig. 6. The main features of these results are readily understandable. When $V_{\rm dc}$ is small each electron bubble that is formed remains in the cell a long time before drifting to the cell wall. Conse-

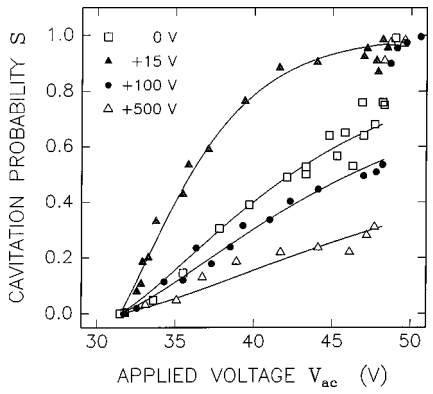

FIG. 6. Cavitation probability S at $T=2.75$ K and saturated vapor pressure as a function of ac voltage V_{ac} applied to the transducer for four different dc voltages V_{dc} as indicated. The solid curves are fits to the data based on Eq. (30).

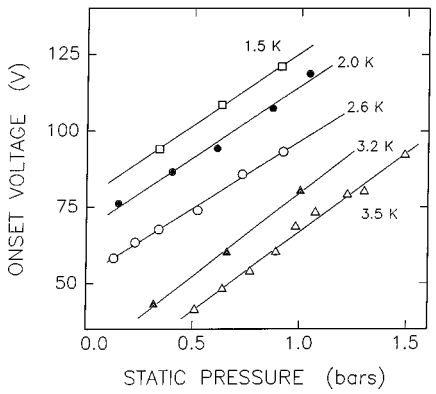

FIG. 7. Onset voltage for nucleation on electrons as a function of the static pressure applied to the liquid. The solid lines are least-squares fits to the data based on the assumption of a linear relation between the pressure swing and the voltage applied to the transducer as described in the text.

quently, the electron density is high. Therefore there is usually at least one electron very close to the acoustic focus, i.e., close to the point in the liquid at which the pressure swing has its maximum amplitude. If this is the case, the probability of cavitation will rise very rapidly as soon as V_{ac} is sufficient to make the pressure swing at the focus exceed the negative pressure that is required to ''explode'' an electron, i.e., to exceed the pressure at which the energy barrier goes to zero. This is the explanation of the onset of $V_{ac}=31.5$ V in Fig. 6. At the onset it is necessary for there to be an electron precisely at the acoustic focus in order to have cavitation; as V_{ac} is increased beyond this point electrons can explode if they are found within some volume near to the focus. The size of this volume v varies with the ratio of V_{ac} to the onset value $V_{ac,onset}$, and the cavitation probability can be written as

$$S=1-\exp[-nv(V_{ac}/V_{ac,onset})], \tag{30}$$

where n is the electron density. We perform an approximate calculation of this volume below. Note that in Eq. (30) it is assumed that the electrons move a negligible distance during the application of the sound pulse. This appears to be a reasonable assumption based on the discussion below.[17]

When a large dc voltage is applied the electron density n in the helium is reduced. As a result, even for V_{ac} as large as twice $V_{ac,onset}$, the cavitation probability remains significantly less than unity. One can then observe a second threshold, at around $V_{ac}=48$ V in Fig. 6, at which homogeneous nucleation begins to occur with appreciable probability. Above this second threshold the cavitation probability is very close to unity.

Although it is not evident in Fig. 4, there is a small but measurable probability of cavitation even when the transducer driving voltage is significantly below the first onset $V_{ac,onset}$. It appears that these ''rare events'' are caused by high-energy electrons which pass through the acoustic focus and deposit energy there at the same time that the sound oscillation is present.

A. Variation of onset voltage with temperature and pressure

We first discuss the threshold for cavitation on electron bubbles. From results such as are shown in Fig. 6, it is straightforward to estimate the transducer voltage at which nucleation on electron bubbles first occurs. The next step is to convert these measured voltages into pressures. We first attempted to achieve this conversion by a measurement of the electrical impedance of the transducer as a function of frequency in the vicinity of the acoustic resonance. In principle, this type of measurement can provide the required information about the electromechanical conversion efficiency of the transducer, thereby enabling the surface displacement of the transducer to be calculated. In practice, however, this calculation cannot be performed reliably. There are several secondary resonances near to the main resonance of the transducer, and these make it impossible to determine the electromechanical coupling coefficients.

Consequently, we have used a different method. We assume that the pressure swing that is produced is linearly proportional to the applied voltage. Then the most negative pressure P_{min} which is produced at the focus must be expressible as

$$P_{min}=-aV_{ac}+P_{stat}, \tag{31}$$

where a is a coefficient which is independent of the driving voltage but which may depend on temperature, and P_{stat} is the static pressure in the liquid. Hence, a measurement of the voltage required to produce cavitation as a function of P_{stat} can fix a value for the coefficient a. Results of $V_{ac,onset}$ as a function of P_{stat} for several temperatures are shown in Fig. 7. Let us suppose, as appears reasonable, that the displacement of the transducer surface per unit applied voltage is independent of the temperature. Since the frequency is also independent of temperature, the surface velocity will also not vary with T. The pressure swing at the transducer surface is the product of the transducer velocity with the acoustic impedance of the liquid. Hence this varies with T as ρc, where c is the sound velocity. The pressure swing at the focus is larger than the pressure swing at the transducer surface by a factor proportional to kR, where k is the sound wave number in the liquid and R_{in} is the inner radius of the transducer. Since k is inversely proportional to c, it follows that the pressure swing at the focus should have the same temperature dependence as

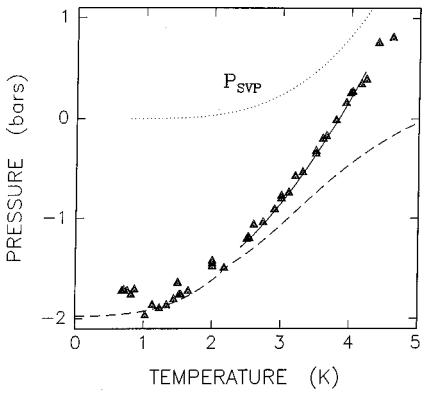

FIG. 8. Comparison of experimental results (solid triangles) for the pressure at which an electron explodes on the PT plane with theory. The dashed line shows the predictions of the simple theory [Eq. (3)], and the solid line is the result obtained when the allowance is made for the finite gas density (see Sec. II D for details). The dotted curve indicates the liquid-vapor coexistence curve.

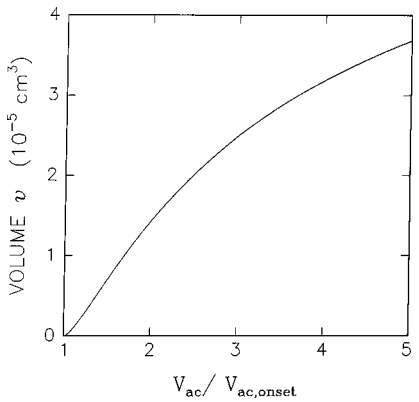

FIG. 9. The volume v in the vicinity of the acoustic focus over which the pressure swing exceeds the voltage required to explode an electron as a function of the applied voltage V_{ac} divided by the onset voltage $V_{ac,onset}$.

the density. Thus we have fit the data in Fig. 7 to Eq. (31) with the coefficient a equal to $b\rho(T)$, where b is a constant independent of temperature.

With this calibration we can then convert the transducer voltage into a pressure swing. In this way we have obtained the results for the explosion pressure as a function of temperature, which are shown in Fig. 8. This is a summary of the data that we have obtained using both transducers and working with different applied rf pulse lengths. Included are the theoretical results for the pressures at which the nucleation barrier for electrons goes to zero. The agreement between theory and experiment is excellent.

B. Variation of the electron density with temperature and electric field

To further analyze the measurements of the cavitation probability as a function of voltage we have calculated the volume v introduced above. We make the simplifying approximation that the transducer is vibrating in a pure radial mode so that the velocity of the inner surface is always normal to the surface and has the same amplitude u_0 at every point. The velocity potential at a point $\vec{r}$ close to the acoustic focus can then be approximated by the expression[18]

$$\psi(\vec{r}) = u_0 \int_{\text{surface}} \frac{e^{iks}}{2\pi s}\, dA, \tag{32}$$

where k is the wave number for the sound ($=\omega/c$), dA is an element of the inner area of the transducer surface, and s is the distance from dA to the point $\vec{r}$. The pressure is then given by

$$P(\vec{r}) = \rho \frac{\partial \psi}{\partial t}. \tag{33}$$

Based on these equations we can calculate the pressure around the acoustic focus, determine the volume over which the pressure swing exceeds any chosen value, and then find the volume $v(V_{ac}/V_{ac,onset})$. This volume for transducer A is shown in Fig. 9. Once this volume is known one can make a fit of Eq. (30) to the data of the type shown in Fig. 6, using the electron density as an adjustable parameter. The solid lines in Fig. 6 are fits of this type.

In this section we restrict our discussion to the results that are obtained for the electron density at temperatures above 1 K. The main features can be summarized as follows. For zero applied dc voltage the electron number density decreases as the temperature goes down, and this decrease becomes very rapid in the lower part of the temperature range. The application of a sufficiently large dc voltage of either sign reduces n. The electron density has its peak value at a positive voltage. As an example, Fig. 10 shows the peak in the density as measured at 2.5 K.

The density of electrons will be determined by a balance between the rate at which electrons are injected by the source and the rate at which they leave the liquid as a result of drift under the influence of electric fields and diffusion. Because of the complex geometry of the transducer region of the cell, it is not possible to make a quantitative calculation of the electron density and its dependence on temperature and applied voltage. The electrons injected by the source have a distribution of energies and hence will have a broad distribution of ranges in the liquid. The mean range in helium for electrons from our source is 0.4 cm. This is comparable to the inner radius of the transducer (0.6 and 0.79 cm for transducers A and B, respectively), and to the distance of the source from the acoustic focus (0.4 cm). As a rough model

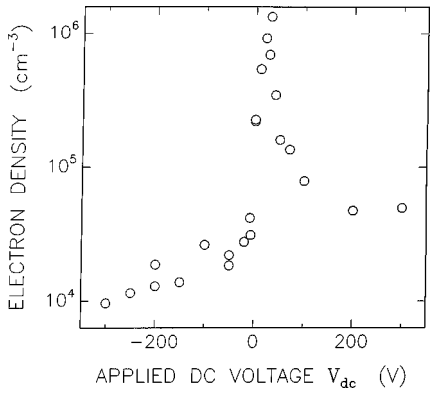

FIG. 10. Measured electron density as a function of the applied dc voltage V_{dc} at $T=2.50$ K and saturated vapor pressure.

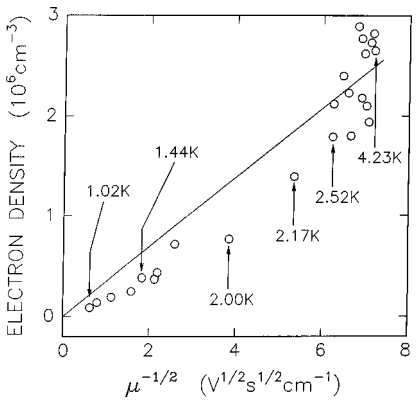

FIG. 11. Plot of electron density versus $\mu^{-1/2}$, where μ is the mobility. These results are taken at saturated vapor pressure with zero dc voltage applied.

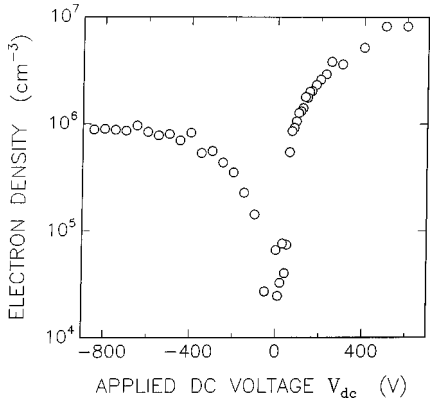

FIG. 12. Measured electron density as a function of the applied dc voltage V_{dc} at $T=0.68$ K and saturated vapor pressure.

we consider the electron density which would result from the injection of electrons at a constant rate per unit volume and time into a hollow sphere of radius R with walls held at ground potential. We first consider the motion of the electrons arising from the space charge field. The result is that the number density n in the steady state is independent of location within the volume and has the value

$$n=\frac{3}{4\pi}\sqrt{\frac{\dot{N}}{\mu e R^3}}, \tag{34}$$

where μ is the mobility of the electron bubbles, and $\dot{N}$ is the total injection rate by the source (3×10^5 s^{-1}). The variation of n with temperature is then determined by the temperature dependence of the mobility μ. We have tested this result by making a plot of n against $\mu^{-1/2}$ using data obtained over the temperature range 1.02 to 4.23 K (Fig. 11). The solid line in Fig. 11 is a linear least-squares fit to the data using R equal to 1.0 cm, and this value appears to be reasonable. However, as can be seen from Fig. 11 the data cannot be fit well by a straight line. It seems likely that this disagreement comes about because the source actually injects a highly inhomogeneous distribution of electrons into the liquid, rather than the uniform distribution assumed in the model. We have not attempted to demonstrate by calculation that this is the explanation.

One can also consider the number density that would result if the space charge field were unimportant and the electrons moved diffusively. The diffusion coefficient D is related to the mobility by the Einstein relation $D=\mu k_B T/e$, and the density in the liquid is then

$$n=\frac{\dot{N}e}{8\pi\mu k_B T}\frac{R^2-r^2}{R^3}. \tag{35}$$

This gives a much larger density at $r=0$ than is obtained from Eq. (34). This indicates that under the conditions of the experiment diffusion is unimportant compared to drift under the influence of the space charge field.

A peak in the electron density as a function of applied voltage V_{dc} (see Fig. 10) is to be expected simply because the electron density must decrease towards zero as the magnitude of the applied voltage increases regardless of the sign. The fact that the peak is at a *positive* voltage suggests that there are more electron bubbles injected in the region below the acoustic focus (i.e., on the source side of the acoustic focus) than above (i.e., adjacent to the transducer). This is as expected based on the energy spectrum of the electrons from the source and the known variation of the range in liquid helium with electron energy.

C. Effects due to vortices at low temperatures

As the temperature is lowered the electron density for zero applied voltage decreases rapidly due to the increase in electron mobility [see Eq. (34)]. The voltage at which the peak occurs also decreases, and at 1.13 K the peak is at $V_{dc}=3$ V. At temperature around 0.9 K the electron density for V_{dc} has become so small that it is hard to detect cavitation events and the peak has become very small. However, at even lower temperature a qualitatively different behavior is seen. There is no peak and the electron density now *increases* with increasing applied voltage of either sign. For example, results of the electron density as a function of applied dc voltage at 0.68 K are shown in Fig. 12. We believe that this behavior is the result of the generation of quantized vortices by the electrons. At 0.68 K the mobility is ~60 cm^2 V^{-1} s^{-1}, and thus for an applied voltage of the order of 100 V it is reasonable to expect that some electrons will reach the critical velocity (3×10^3 cm s^{-1}) that is required for the production of vortices. Electrons trapped on vortex rings move very slowly, with a velocity that decreases with increasing energy, and hence a high electron density should result. Above 1 K the mobility is reduced and electrons do not produce vortices for the highest applied dc voltages which liquid helium can sustain without sparkling.

This interpretation is supported by a measurement of the threshold voltage for nucleation. We find that this voltage is approximately 12% *less* at 0.68 K than it is at 1.02 K. This change is thus in the opposite direction from the $\sim2\%$ change that would be expected to arise from the variation of the surface tension with temperature. The theory given in Sec. II predicts a 4% decrease in the instability pressure when an electron bubble is attached to a vortex; the measurements indicate that this reduction is 14% and thus imply that a more detailed and quantitative theory, possibly based on a density-functional method, is needed.

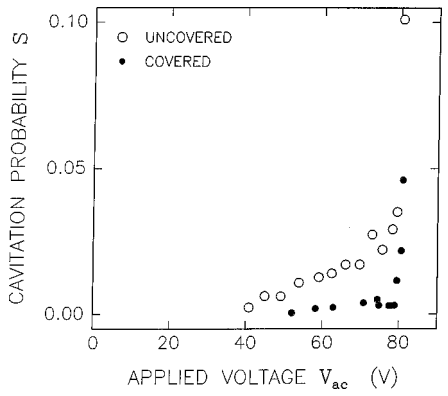

FIG. 13. Cavitation probability S as a function of transducer driving voltage V_{ac} at $T=3$ K and saturated vapor pressure showing the ''rare events.'' Electron bubbles explode when the voltage exceeds 80 V and give rise to the sharp rise in the probability beginning at this voltage. The solid circles are data taken when the compass needle is rotated to block the line-of-sight between the radioactive source and the acoustic focus.

D. ''Rare events''

We now discuss the small number of events which can be detected for applied voltages below the threshold voltage. When measurements are made with the ultrasonic transducer operating in the thickness mode at 560 kHz or 1.4 MHz, the probability associated with these events is typically a few percent, or less. These events cannot be explained by nucleation on electron bubbles. The events extend to voltages as low as one half the threshold voltage, at which point the energy barrier for nucleation from an electron bubble is extremely large. Figure 13 shows data taken with transducer A at 560 kHz.

An explanation of the origin of these events must take account of the following observations:

(1) The probability is unaffected by the application of dc electric fields.

(2) We attached a small plate to a compass needle and placed it so that it could swing in the region between the source and the acoustic focus. The needle could be moved by application of a magnetic field so that the plate blocked the line of sight between the focus and all points on the surface of the source. When the plate was moved so that it was between the source and the focus the rate of the rare events was decreased by a large factor (see Fig. 13).

(3) The probability of cavitation S increased with the amount of time over which the sound pulse was applied. This contrasts with results for the nucleation processes studied above the threshold. These do not depend on the duration of the sound pulse [see Eq. (30)].

These results suggest that the rare events may be caused by electrons from the source which move through the acoustic focus at high speed before they have lost their kinetic energy and become trapped as bubbles. If one of these electrons deposit sufficient energy at a point within the focal region while the sound wave is present, nucleation can occur. Thus, this is the same type of nucleation as occurs in a bubble chamber.

This interpretation is consistent with the observations listed above. The kinetic energy of the electrons coming from the source is typically several hundred keV and so the path of these electrons is unaffected by the application of small static electric fields. The thickness of the plate attached to the compass needle was sufficient to absorb nearly all the electrons coming from the source and so should substantially reduce the number of electrons passing through the focus. The probability of cavitation should be proportional to the rate at which energetic electrons pass through the focus and to the time that the sound wave is present.

These events are difficult to study because the cavitation probability is so low. We have made measurements, and detected nucleation events, down to transducer drive voltages as low as about half the voltage that is required to explode electron bubbles. Below this voltage the probability is very small, less than $\sim 10^{-3}$, and consequently is very hard to measure. One way to increase the probability is to use a lower sound frequency so that the size of the acoustic focus is increased. This then makes it more probable that an electron will pass through the active region during the time of the sound pulse. When the sound is generated by means of a transducer operated in the thickness mode it is not practical to significantly lower the frequency. Consequently, we instead used the 137 kHz flexural mode of transducer B. This gives a much larger focal region and the number of ''rare events'' is indeed found to be greatly increased. The data obtained in this way indicate that there is a threshold voltage below which no events occur.

Nucleation in helium bubble chambers has been discussed in detail in a number of review articles.[19–21] Along the track a large number of ionization processes occur resulting in the production of δ rays, i.e., recoiling secondary electrons. These δ rays have a continuous spectrum of energies up to a cutoff. The consensus appears to be that the bubbles that are seen in bubble chambers come from δ rays whose energy lies in the upper part of the energy spectrum. However, no quantitative theory of the probability that a δ of given energy will nucleate a bubble is available, and consequently we have not attempted to make a detailed analysis of the variation of the probability of the rare events with transducer driving voltage.

ACKNOWLEDGMENTS

This work was supported in part by the National Science Foundation through Grant No. DMR 91-20982 and by the Alexander von Humboldt Foundation. The authors would like to thank S. Hall and M. S. Pettersen for help with the experiment and S. Balibar for several helpful discussions.

*Present address: Institut für Angewandte Physik, Universität Heidelberg, Germany.

†Present address: Department of Physics and Astronomy, University of Delaware, Newark, Delaware 19716.

[1] H. J. Maris, S. Balibar, and M. S. Pettersen, J. Low Temp. Phys. **93**, 1069 (1993).

[2] M. S. Pettersen, S. Balibar, and H. J. Maris, Phys. Rev. B **49**, 12 062 (1994).

[3] H. J. Maris, in *Proceedings of the 21st International Conference on Low Temperature Physics*, Prague, August 1996 [Czech. J. Phys. **46**, Suppl. S6, 2943 (1996)].

[4] H. J. Maris, J. Low Temp. Phys. **98**, 403 (1995).

[5] S. Balibar, C. Guthmann, H. Lambare, P. Roche, E. Rolley, and H. J. Maris, J. Low Temp. Phys. **101**, 271 (1995).

[6] H. Lambare, P. Roche, E. Rolley, S. Balibar, C. Guthmann, and H. J. Maris, in *Proceedings of the 21st International Conference on Low Temperature Physics*, Prague, August 1996 [Czech. J. Phys. **46**, Suppl. S1, 383 (1996)].

[7] H. J. Maris, J. Low Temp. Phys. **94**, 125 (1994).

[8] S. C. Hall, J. Classen, C. K. Su, and H. J. Maris, J. Low Temp. Phys. **101**, 793 (1995).

[9] J. Classen, C. K. Su, and H. J. Maris, Phys. Rev. Lett. **77**, 2006 (1996).

[10] W. T. Sommer, Phys. Rev. Lett. **12**, 271 (1964); M. A. Woolf and G. W. Rayfield, *ibid.* **15**, 235 (1965).

[11] For a review, see A. L. Fetter, in *The Physics of Liquid and Solid Helium*, edited by K. H. Benneman and J. B. Ketterson (Wiley, New York, 1960).

[12] For consistency with the density-functional calculation we have used the value 0.3544 erg cm^{-2} measured by M. Iino, M. Suzuki, and A. J. Ikushima, J. Low Temp. Phys. **61**, 155 (1985), rather than the value of 0.375 erg cm^{-2} obtained from the more recent measurements of G. Deville, P. Roche, N. J. Appleyard, and F. I. B. Williams, Czech. J. Phys. **46**, Suppl. S1, 89 (1996).

[13] L. B. Lurio, T. A. Rabedeau, P. S. Pershan, I. F. Silvera, M. Deutsch, S. D. Kosowsky, and B. M. Ocko, Phys. Rev. B **48**, 9644 (1993). This width is the distance over which the density changes from 10 to 90% of its bulk value.

[14] S. C. Hall and H. J. Maris, J. Low Temp. Phys. **107**, 263 (1997).

[15] R. J. Donnelly and P. H. Roberts, Proc. R. Soc. London, Ser. A **312**, 519 (1969).

[16] Channel Industries, Inc., 839 Ward Drive, Santa Barbara, California 93111.

[17] The time for an electron bubble to leave the cell is typically of the order of 1 s, and thus the electron velocity is ~ 1 cm s^{-1}. Hence, for a sound pulse of duration 100 μs an electron will only move 1 μm, which is significantly less than the linear dimensions of the acoustic focus. It is possible, however, that the sound field itself produces a flow of the liquid which moves electrons through the focal region.

[18] H. T. O'Neil, J. Acoust. Soc. Am. **21**, 516 (1949).

[19] F. Seitz, Phys. Fluids **1**, 2 (1958).

[20] A. G. Tenner, Nucl. Instrum. Methods **22**, 1 (1963).

[21] *Bubble and Spark Chambers*, edited by R. P. Shutt (Academic, New York, 1967); Yu. A. Aleksandrov, G. S. Voronov, V. M. Gorbunkov, N. B. Delone, and Yu. I. Nechayev, *Bubble Chambers* (Books on Demand, Ann Arbor, MI, 1967).